

Theoretical Investigation of the C₆₀/Copper Phthalocyanine Organic Photovoltaic Heterojunction

Jun Ren^{1,2}, Sheng Meng³ (✉), and Efthimios Kaxiras⁴

¹ State Key Laboratory for Low-Dimensional Quantum Physics, Department of Physics, Tsinghua University, Beijing 100084, China

² Institut des Matériaux, École Polytechnique Fédérale Lausanne (EPFL), CH-1015, Lausanne, Switzerland

³ Beijing National Laboratory for Condensed Matter Physics, and Institute of Physics, Chinese Academy of Sciences, Beijing 100190, China

⁴ Department of Physics and School of Engineering and Applied Sciences, Harvard University, Cambridge MA 02138, USA

Received: 9 November 2011 / Revised: 31 January 2012 / Accepted: 1 February 2012

© Tsinghua University Press and Springer-Verlag Berlin Heidelberg 2012

ABSTRACT

Molecular heterojunctions, such as the one based on copper phthalocyanine (CuPc) and carbon fullerene (C₆₀) molecules, are commonly employed in organic photovoltaic cells as electron donor–acceptor pairs. We have investigated the different atomic structures and electronic and optical properties of the C₆₀/CuPc heterojunction through first-principles calculations based on density functional theory (DFT) and time-dependent DFT. In general, configurations with the CuPc molecule “lying down” on C₆₀ are energetically more favorable than configurations with the CuPc molecule “standing up”. The lying-down configurations also facilitate charge transfer between the two molecules, due to the stronger interaction and the larger overlap between electronic wavefunctions at the interface. The energetically preferred structure consists of CuPc placed so that the Cu atom is above a bridge site of C₆₀, with one N–Cu–N bond of CuPc being parallel to a C–C bond of C₆₀. We also considered the structure of a periodic CuPc monolayer deposited on the (001) surface of a face-centered cubic (fcc) crystal of C₆₀ molecules with the lying-down orientation and on the (111) surface with the standing-up configuration. We find that the first arrangement can lead to larger open circuit voltage due to an enhanced electronic interaction between CuPc and C₆₀ molecules.

KEYWORDS

Organic solar cell, heterojunction, interface, ab initio, time-dependent density functional theory

1. Introduction

Organic photovoltaic (OPV) cells are the subject of increasing attention as a promising alternative to established inorganic technologies, because of several advantages such as low cost, easy fabrication, excellent flexibility, and compatibility with large-area substrates [1–3]. The operation of these cells is based on the concept of the electron donor–acceptor (D–A)

heterojunction [4]. By means of exploring several options that affect performance—including doping, using tandem cells, inserting buffer layers between the active layer and anode, and employing highly purified fullerenes—the power conversion efficiency of OPV cells has recently reached the level of 5–6% [2, 5–10]. The precise control of the morphology and fine-tuning of the electronic structure can play a crucial role in enhancing the performance of OPV

Address correspondence to smeng@iphy.ac.cn

cells [11]. Accordingly, a detailed understanding of the atomic-scale features of the heterojunction interface and their effects on the electronic and optical properties are of paramount importance in improving the stability and efficiency of these devices.

In high efficiency devices, a common choice is to use copper phthalocyanine (CuPc) as a p-type molecular semiconductor and carbon fullerenes (C_{60}) as an n-type semiconductor, for the electron donor and electron acceptor components, respectively. The molecular orientation of CuPc on C_{60} [12, 13], the corresponding band alignment [14, 15], and the ultrafast charge transfer at the CuPc/ C_{60} interface [16] have been extensively investigated from the experimental point of view, but the atomic structure and the interaction between CuPc and the C_{60} thin film are not well understood at the atomic scale. In particular, the molecular arrangement of CuPc on C_{60} , which determines the charge transfer at the interface, is still unclear.

The stabilities of the lying-down and the standing-up configurations of CuPc on C_{60} depend on coverage. At low coverage, namely a fraction of a monolayer of CuPc, when the CuPc molecules are deposited on a Au(111) surface covered by a monolayer of C_{60} , they prefer to lie flat on the surface [13], because of the larger contact area and the stronger electronic interaction between CuPc and C_{60} molecules. This is also the case for the structure of CuPc molecules on graphite [17], Ag(111) [12, 18], Cu(111) [19], and $TiO_2(011)-(2 \times 1)$ surfaces [20]. In addition, CuPc molecules adopt a square lattice pattern in a lying-down configuration when deposited on the C_{60}/MoS_2 system [21]. At high coverage, namely a monolayer or more of CuPc, adsorption of CuPc on $C_{60}/Ag(111)$ leads to a thin film in which the CuPc molecules assume a standing-up configuration on top of the C_{60} monolayer [12], because of the stronger interaction between CuPc molecules and the weaker interaction between CuPc and C_{60} . The difference between the lying-down and standing-up orientations of the CuPc molecules depends on the strength of the interaction between the molecules and the interaction of each molecule with the surface. The arrangement of molecules on the CuPc layer also depends strongly on whether the molecular CuPc and C_{60} lattices are commensurate or not. Scanning tunneling microscopy (STM) images indicate that a C_{60} monolayer forms a hexagonal lattice on the

Si(111)- (7×7) surface, and a square lattice with a $c(4 \times 4)$ ordering on the Si(100)- (2×1) surface [22]. The nearest neighbor distances between C_{60} molecules are 10.2 Å and 10.9 Å for the hexagonal and square lattices, respectively, while in crystalline C_{60} , the nearest neighbor distance is 10.02 Å [23]. These comparisons suggest a better fit of the C_{60} monolayer on the Si(111)- (7×7) surface than on the Si(100)- (2×1) surface. These considerations are useful in choosing the right substrate for the deposition of a CuPc layer on top of an ordered layer of C_{60} molecules for the formation of the heterojunction.

In the present work, we present a theoretical investigation of the atomic structure and the resulting electronic and optical properties of the CuPc/ C_{60} molecular complexes in various configurations. We use first-principles calculations based on density functional theory (DFT) and time-dependent DFT (TDDFT). After optimizing the atomic structures, we find that the CuPc molecule prefers to lie on the C_{60} molecule with the Cu atom above a bridge site of C_{60} so that one N–Cu–N bond is parallel to a C–C bond of C_{60} , with standing-up configurations generally being higher in energy. In addition, the lying-down configurations exhibit a stronger electron polarization effect at the CuPc/ C_{60} interface and 0.3 eV higher open circuit voltage than the standing-up orientations. The electronic and optical properties are also distinct in the two different types of molecular arrangement. Using the energetically favored structures of the CuPc/ C_{60} complex, we extend our investigations to the simulation of the CuPc/ C_{60} thin film heterojunction, by considering two types of arrangements, namely a CuPc/ C_{60} (001) structure with CuPc molecules in lying-down configuration, and a CuPc/ C_{60} (111) structure with CuPc molecules in standing-up configuration. Based on results from these model systems, we predict that the former type of heterojunction will exhibit a higher efficiency for charge transfer due to the stronger electronic interaction, which can lead to larger open circuit voltage in the photovoltaic device.

2. Computational methods

Our theoretical study is based on first-principles calculations in the framework of DFT. We used



pseudopotentials of the Troullier–Martins type [24] to model the atomic cores, the Ceperley–Alder form of the local density approximation (LDA) as the exchange–correlation functional [25], and a local basis set of double- ζ polarized orbitals (13 orbitals for C and N, and 5 orbitals for H) as implemented in the SIESTA code [26]. We also used van der Waals–density functionals (vdW-DF) of the Lunqvist–Langreth type for typical bonding configurations [27], because vdW forces dominate the interaction between the two molecular components. An auxiliary real space grid equivalent to a plane-wave cutoff of 120 Ry and the Γ point was used to optimize the geometry. In addition, spin polarization of electronic orbitals was taken into account. For geometry optimization, structures were allowed to fully relax until forces on the atoms were smaller in magnitude than 0.04 eV/Å. The basis set superposition error (BSSE) was excluded when calculating the binding energies. For optical absorbance spectrum calculations within TDDFT in the linear response regime [28], we used 6107 steps in time to propagate the wavefunctions with a time step of 3.4×10^{-3} fs, which gives an energy resolution of 0.1 eV. The perturbing external electric field was 0.1 V/Å.

For the CuPc/C₆₀ thin film periodic structures, we considered two kinds of supercells composed of a monolayer of fullerene and CuPc molecules with a separating vacuum layer exceeding 10 Å. For the lying-down molecular orientation, we adopted a square lattice with lattice constant 14.17 Å to simulate the

CuPc/C₆₀ (001) system, in a unit cell containing two C₆₀ molecules and one CuPc molecule. For the standing-up orientation, a hexagonal lattice with lattice constant 10.02 Å was chosen to simulate the CuPc/C₆₀ (111) system, in a unit cell that contains one C₆₀ and one CuPc molecule.

3. Results and discussion

3.1 CuPc/C₆₀ molecular complex

We begin by considering the different molecular complexes composed of a single CuPc and a C₆₀ molecule. We define the adsorption site as the projection of the central Cu atom of CuPc on the C₆₀ structure. We investigated four different adsorption sites for CuPc lying down on C₆₀, including the center of a hexagon (labeled L_h), a C atom of a hexagon with the hexagon parallel to the CuPc plane (L_c), the bridge site (L_b) between two C atoms, and a C atom at the apex of two hexagons and one pentagon (L_a). We also considered two standing-up configurations: in the first, the center of CuPc is directly above the center of a C₆₀ hexagon (labeled S_h) while in the second it is directly above the bridge site between two C atoms of C₆₀ (S_b). All these configurations are shown in Figs. 1(a)–1(f). The binding energies and salient structural features of the optimized geometries for these configurations are given in Table 1.

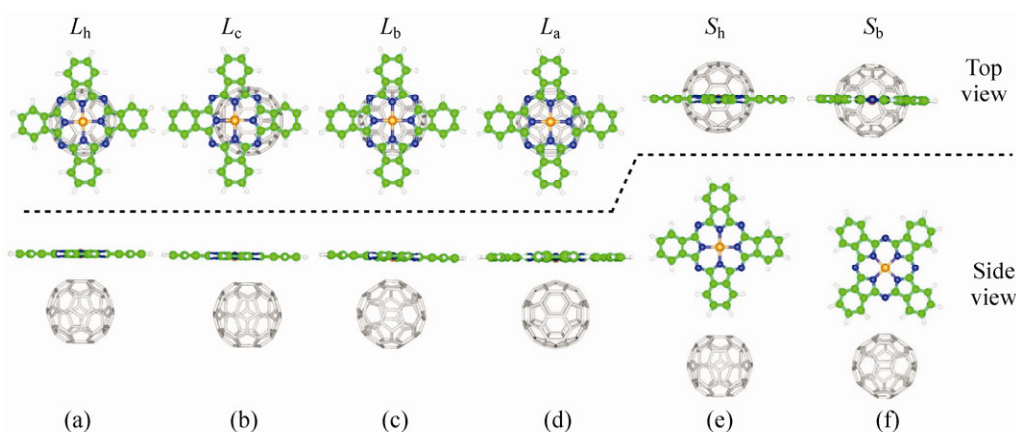


Figure 1 Different configurations for CuPc adsorption on a C₆₀ surface: L_h , L_c , L_b , and L_a represent the distinct lying-down orientations; S_h and S_b represent the standing-up orientations. A top view (above dashed line) and side view (below dashed line) are shown for each configuration. C, H, N and Cu atoms in CuPc are denoted as green, white, blue and orange spheres, respectively. Only the bonds between C atoms in C₆₀ are shown as grey lines

Table 1 Calculated binding energies (in eV) and adsorption height (in Å) of CuPc from C₆₀ molecules for the various lying-down and standing-up configurations shown in Fig. 1. The quantities denoted by a prime correspond to calculations that include the vdW contribution to the energy and forces (see text for details)

Geometry	E_b	E'_b	$d_{\text{Pc-C}_{60}}$	$d'_{\text{Pc-C}_{60}}$
L_h	-0.27		3.04	
L_c	-0.33		2.98	
L_b	-0.37	-0.65	2.64	2.94
L_a	-0.37	-0.64	2.59	2.89
S_h	-0.11		2.53	
S_b	-0.17	-0.22	2.36	2.71

The binding energies are defined as

$$E_b = (E_{\text{tot}} - n(E_{\text{C}_{60}} + E_{\text{Pc}}))/n \quad (1)$$

where E_{tot} , $E_{\text{C}_{60}}$ and E_{Pc} are the total energy of the complex, the energy of the isolated C₆₀ molecule, and the energy of gas-phase CuPc molecule, respectively; and n is the number of CuPc and C₆₀ molecules in a unit cell. The binding energy denoted as E'_b includes the vdW contribution, as described in the Computational methods section; all energies include the BSSE correction. The adsorption height $d_{\text{Pc-C}_{60}}$ (and the corresponding value $d'_{\text{Pc-C}_{60}}$ which includes the vdW contribution to the forces), for the lying-down configurations, corresponds to the distance from the Cu atom in CuPc to the closest atom in C₆₀, or the average of the distance to the closest set of C atoms, along the line connecting the center of C₆₀ to the Cu atom. For the standing-up configurations, these distances correspond to the average distance of the H atoms on CuPc to the closest atoms on C₆₀, along the same line. As seen from these results, the lying-down configurations are energetically preferred over the standing-up ones. Inclusion of vdW energy and force contributions make the binding energies lower, as expected after taking into account additional attractive interactions, but make the distance between the two molecules larger, by ~0.3 Å. The lowest energy structure, L_b , is the one in which the Cu atom of CuPc lies directly above the center of a C–C bond of C₆₀, with one N–Cu–N bond being parallel to the C–C bond of the C₆₀ molecule. The two configurations in which the Cu atom of CuPc lies directly above a C atom of C₆₀, namely L_a and L_c , are very close in energy to L_b . Only

the configuration in which the Cu atom of CuPc lies directly above the center of a hexagonal ring of C₆₀ has a significantly higher energy, by about 0.1 eV, and has the two molecules farther apart. A similar geometry is found for the ZnPc/C₆₀ system [29].

The stability of these structures is determined by maximizing the atom-to-atom contact between the CuPc and C₆₀ molecules. Since CuPc is a planar molecule while C₆₀ is spherical, Cu (the center of CuPc) binding onto a flat hexagon of C₆₀ (configurations L_h and L_c) would have only this hexagon in effective good contact with CuPc. In contrast to this, placing the Cu atom of CuPc directly above the vertex C atom (L_a) and the C–C bridge (L_b) of C₆₀ maximizes the contact of CuPc with three or four aromatic rings, thus leading to larger binding energies. Moreover, the four-fold symmetry of CuPc would facilitate Cu binding on top of the C–C bridge with one N–Cu–N bond aligned with a C–C bond to maximize the close immediate contact of four aromatic rings with CuPc (shown in Fig. 1). This makes the L_b configuration the most stable. As a result of these interactions, the lying-down configurations are energetically preferred over the standing-up ones: the interaction energy is ~3 times larger in the former. To summarize, we note that the average atom-to-atom distance between CuPc and C₆₀ is much smaller in the lying-down configurations than in the standing-up ones, namely, more atoms are within the effective van der Waals radii of the other molecule, resulting a larger effective contact area and stronger attraction between the two molecules.

To shed some light onto the nature of the interaction between CuPc and C₆₀, we calculated the corresponding charge density difference (CDD), $\Delta\rho$, shown in Figs. 2(a) and 2(b), which gives clues as to the bonding character and charge redistribution after adsorption of a CuPc molecule on C₆₀. The definition of $\Delta\rho$ is

$$\Delta\rho = \rho_{\text{tot}} - \rho_{\text{C}_{60}} - \rho_{\text{Pc}} \quad (2)$$

where ρ_{tot} , $\rho_{\text{C}_{60}}$ and ρ_{Pc} are the charge densities of the molecular complex, the isolated C₆₀, and the CuPc molecule, respectively, with geometries fixed at the optimized ones in the complex. In general, the lying-down configurations lead to more pronounced charge transfer between CuPc and C₆₀ than in the case of the standing-up orientations. Specifically, in the lying-down



orientation, more electrons accumulate in the region between the two molecules, especially for configurations L_b and L_a than for the standing-up orientations, as seen in Figs. 2(a) and 2(b).

To quantify these effects, we integrated the CDD on planes perpendicular to the line connecting the center of C_{60} to the Cu atom of CuPc (referred as the “z” direction), which gives the planar averaged CDD, $\Delta\rho_z$

$$\Delta\rho_z = \int \rho(x, y, z) dx dy \quad (3)$$

shown in Figs. 2(c) and 2(d). From the planar averaged CDD, it is clear that the CDD magnitude for the lying-down molecular orientations is more than a factor of two larger than for the standing-up orientations, indicating stronger electron polarization for the lying-down configurations, which leads to enhanced electronic interaction between CuPc and C_{60} . We note that the CCD defined here may not directly account for charge transfer upon excitation, which is a complicated process involving many parameters including the excitation energy cost and electronic couplings. Here the CCD is linked to electronic coupling strength at

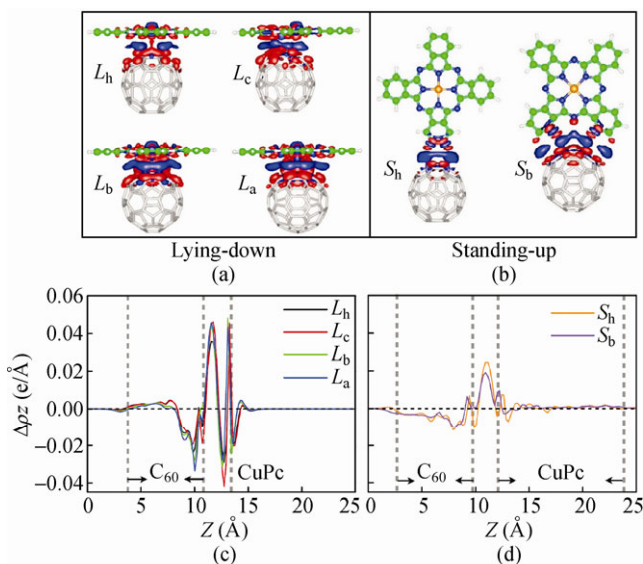


Figure 2 Side view of the charge density difference for: (a) the lying-down CuPc/ C_{60} configurations and (b) the standing-up geometries; constant $\Delta\rho$ contour levels are at $0.03 \text{ e}/\text{\AA}^3$, with the blue and red clouds corresponding to regions of electron accumulation and depletion. The planar averaged charge density difference along the C_{60} –CuPc direction for: (c) the lying-down configurations and (d) the standing-up ones. The dashed vertical lines in (c) and (d) mark the regions occupied by the CuPc and the C_{60} molecules

the interface; larger values imply stronger electron interaction and polarization, which favors exciton dissociation and charge separation due to the presence of interface dipole. Precise determination of the charge transfer rate in excited states requires time-dependent simulations of excited states, which are currently being carried out.

In the context of OPV heterojunctions, it is of great interest to obtain the optical absorbance spectra of the various molecular arrangements. To this end, we concentrate on the two lowest-energy complexes, namely L_b and S_b , and compare their features to those of the individual molecules. The results are shown in Fig. 3. It is clear that both lying-down and standing-up configurations show two major absorbance bands, in the range 610–650 nm for the band labeled Q and 300–420 nm for the band labeled B. These are the same bands as those of the isolated CuPc molecule, with relatively small changes. Only one band of C_{60} lies in the range of the B band of CuPc, and its effect is to produce slight changes in the position of the B band peaks of CuPc, especially in the L_b configuration. For a more detailed analysis, we fitted the calculated spectra in each case by a superposition of Lorentzian functions with their positions, heights, and widths as free parameters. The positions of the peaks obtained by this

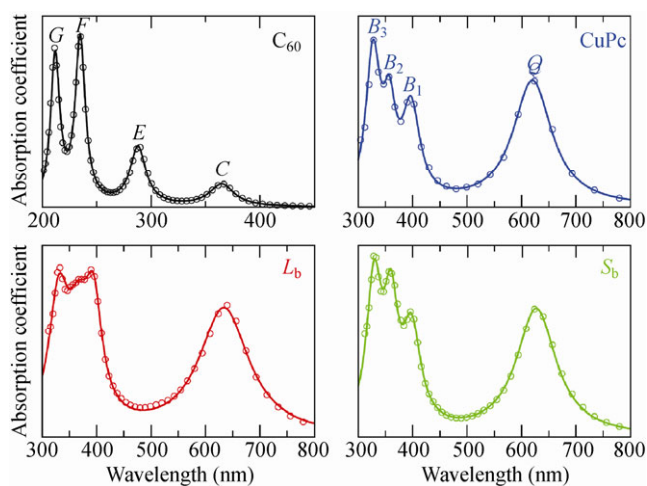


Figure 3 Optical absorption spectra of the isolated C_{60} (black) and CuPc (blue) molecules, and of the two most favorable complexes, L_b (red) and S_b (green), as calculated from TDDFT. The points in each case are the calculated values and the lines are fits of a superposition of Lorentzian functions with variable height, position and width

procedure are given in Table 2; these results are in reasonable agreement with the primary peaks measured in UV-vis spectra for both isolated molecules [23, 30].

To elucidate the nature of the absorption peaks, we analyzed the electronic structure of the most stable configurations, namely L_b and S_b . The energy level diagram for L_b is shown in Fig. 4, along with wavefunctions for representative states. In this CuPc/ C_{60} complex, the highest fully occupied molecular orbital (HOMO) is localized on CuPc, while the lowest unoccupied molecular orbital (LUMO) is localized on C_{60} . The highest occupied and the lowest unoccupied states of CuPc are actually composed of a single-spin orbitals (SOMO and SUMO), which are identified by up and down arrows in Fig. 4 and are usually denoted as $b_{1g\uparrow}$ and $b_{1g\downarrow}$, respectively. The respective fully occupied HOMO is a single a_{1u} level with two electrons, while the second unoccupied CuPc level is an e_g doubly-degenerate state. The HOMO and LUMO states of C_{60} comprise five-fold degenerate, fully occupied states, and three-fold degenerate states, respectively; in CuPc/ C_{60} , the five-fold degeneracy of the C_{60} -HOMO is broken due to lower symmetry, into a three-fold and a two-fold degenerate level. The gap between the CuPc-SOMO and the C_{60} -LUMO levels for the L_b configuration is 0.92 eV, consistent with the experimental result of 1.03 eV [14]. For the S_b configuration of the CuPc/ C_{60} complex, the overall arrangement of energy levels is the same, but the gap between occupied and unoccupied states is smaller, resulting from an approximately rigid translation of the CuPc energy levels to higher values relative to the C_{60} levels. Specifically, the gap between the CuPc-SOMO and the C_{60} -LUMO levels for

Table 2 The main features in the optical absorption spectra of the C_{60} and CuPc molecules (in nm) in isolated form or within the CuPc/ C_{60} system in the lowest-energy lying-down (L_b) and standing-up (S_b) configurations

	<i>C</i>	<i>E</i>	<i>F</i>	<i>G</i>	
C_{60}	365	288	235	212	
(Exp. [31])	(330)	(270)	(230)	(210)	
	<i>X</i>	<i>Q</i>	<i>B</i> ₁	<i>B</i> ₂	<i>B</i> ₃
CuPc	620	397	357	327	
CuPc/ C_{60} : L_b	1230	634	395	367	330
CuPc/ C_{60} : S_b	1550	627	398	360	329

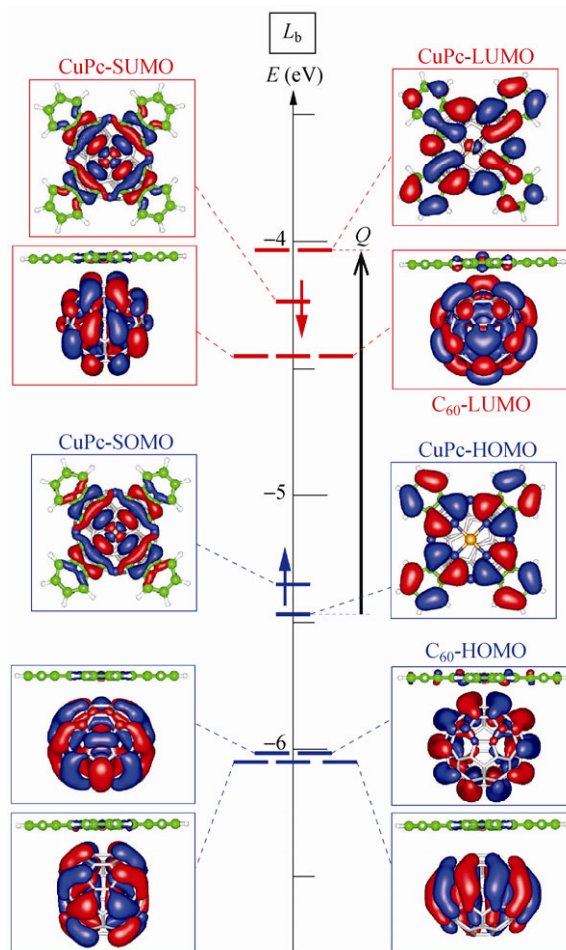


Figure 4 Energy of individual electronic states of the CuPc/ C_{60} complex in the lying-down configuration L_b . The vertical axis is the energy in eV, with individual levels denoted by horizontal bars, with blue for occupied and red for unoccupied levels. All states are occupied by a pair of opposite spin electrons, except for those denoted by an up or down arrow, indicating single-spin occupancy. Wavefunctions of representative levels are also shown, with blue and red clouds corresponding to positive and negative values. The states that correspond to the lowest unoccupied and highest occupied molecular or spin orbitals are labeled in each case. The vertical arrow indicates transitions that contribute to the Q band in optical absorption

the S_b configuration is 0.63 eV, or 0.3 eV smaller than in the L_b configuration, which indicates that a larger open circuit voltage would be obtained in the lying-down configuration. Taking also into consideration the stronger coupling between CuPc and C_{60} and the larger electron polarization in the lying-down configuration, as discussed earlier, we conclude that this type of arrangement is more favorable for exciton dissociation at the Pc/ C_{60} interface.



It is worth pointing out that the lowest energy (highest wavelength) absorption band corresponding to the transition between the CuPc-SOMO and the C_{60} -LUMO states of the CuPc/ C_{60} complex is around 1230 nm for L_b and 1550 nm for S_b . These features appear as weak shoulders in the calculated optical absorption spectra (not shown in Fig. 3) and are labeled the X band in Table 2, because they are extra bands due to the formation of the complex. However, these absorption bands would be difficult to detect in experiments, due to very small intensity. As a result, the bands labeled Q at 634 nm for the L_b configuration and 627 nm for the S_b configuration correspond to the electronic transition from the HOMO to the LUMO state of CuPc molecule, as indicated in Fig. 4.

3.2 CuPc/ C_{60} thin film heterojunction

In the formation of the molecular heterojunction, the arrangement of the C_{60} monolayer on the substrate and the lattice mismatch between CuPc and C_{60} are critical factors that influence the CuPc molecular orientation on C_{60} . Recently, scanning tunneling microscopy images have revealed that CuPc molecules adopt a standing-up molecular orientation on a C_{60} monolayer deposited on Ag(111) [12]. It is clear that the C_{60} monolayer forms a close-packed hexagonal lattice, that is, the equivalent of a $C_{60}(111)$ crystal surface, when deposited on Ag(111). Based on STM images [32], C_{60} forms a uniform close-packed hexagonal ($2\sqrt{3} \times 2\sqrt{3}$) $R30^\circ$ structure, when deposited on Ag(111). The C_{60} spacing is 10 Å, which is the same as the spacing between molecules on the C_{60} face-centered cubic (fcc) (111) crystal surface. The large lattice mismatch between the CuPc monolayer with the lying-down molecular orientation and the $C_{60}(111)$ surface precludes the possibility of the lying-down orientation for CuPc adsorption on this surface. Although the $C_{60}(111)$ surface is the commonly observed plane in experiments, on the Si(100)-(2 × 1) and MoS₂ substrate, C_{60} molecules form a square lattice with $c(4 \times 4)$ ordering [21, 22], that is, a supercell of the $C_{60}(001)$ surface. The $C_{60}(001)$ surface offers a good chance for forming a CuPc monolayer on it with the lying-down orientation. Accordingly, we have investigated the possibility of creating a monolayer of CuPc on top of a $C_{60}(100)$

layer in the lying-down configuration and on top of a $C_{60}(111)$ layer in the standing-up configuration. Using the optimized structures of the CuPc/ C_{60} molecular complexes (L_b and S_b), we considered two kinds of supercells with periodic boundary conditions:

- (i) For the lying-down molecular orientation, we adopted a square lattice with the lattice constant 14.17 Å to simulate the CuPc/ $C_{60}(001)$ system, with each unit cell containing two C_{60} molecules and one CuPc molecule, as shown in Fig. 5(a).
- (ii) For the standing-up orientation, we adopted a hexagonal lattice with lattice constant 10.02 Å to simulate the CuPc/ $C_{60}(111)$ system. Only one C_{60} and one CuPc molecule is included in each unit cell, as depicted in Fig. 5(b).

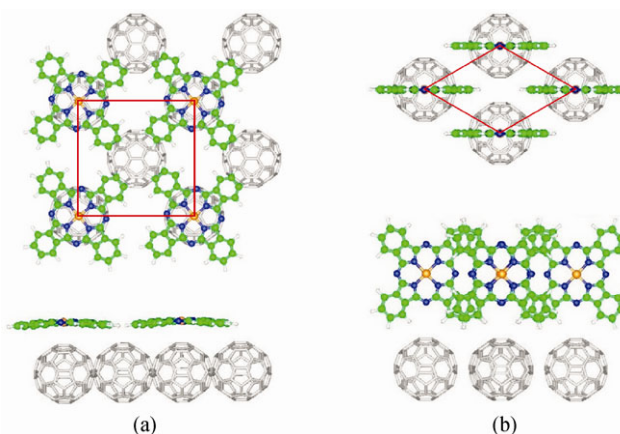


Figure 5 Top view and side view of the geometry of the CuPc/ C_{60} thin film heterojunction: (a) CuPc molecules deposited on the $C_{60}(001)$ surface with the lying-down configuration, in a $\sqrt{2} \times \sqrt{2}$ pattern on the square lattice formed by the C_{60} molecules; (b) CuPc molecules deposited on the $C_{60}(111)$ surface with the standing-up configuration, in a 1×1 pattern on the hexagonal lattice formed by the C_{60} molecules. The unit cell in each case is outlined by red lines

A vacuum layer for both configurations in excess of 10 Å is used to separate the molecular bilayers. The average height between the CuPc and C_{60} layers is 2.812 Å and 2.363 Å for the lying-down and standing-up configurations, respectively, and the corresponding interaction energies between CuPc and C_{60} layers are -0.33 and -0.15 eV/ C_{60} (these values include the BSSE correction, as in the case of the molecular complexes, but not the vdW contribution, which is computationally challenging for the larger unit cells of the periodic

structures). On $C_{60}(001)$ the binding energy of the lying-down configuration is approximately two times larger than that of the standing-up configuration at low coverage, suggesting a more stable configuration of CuPc adsorption on the $C_{60}(001)$ surface. This result is consistent with the trend of the stability for the isolated CuPc/ C_{60} complex. On $C_{60}(111)$ at a higher CuPc coverage, the standing-up configuration is much more stable when the high interaction energy between CuPc molecules (~ 1 eV) is taken into account, which explains the experimental findings on $C_{60}/Ag(111)$ [12].

Since the lying-down configuration has more advantages over the standing-up structure, we focus on the CuPc adsorption upon $C_{60}(001)$ surface. The energy levels of this configuration are essentially the same as in the case of the molecular complex, the only significant difference being that there are twice as many C_{60} -derived states in the periodic structure which contains two C_{60} molecules per unit cell. Interaction between these molecules further breaks the symmetry and reduces the degeneracy of the corresponding electronic levels. Specifically, at the Γ point (the center of the Brillouin zone) the valence band maximum is composed of the SOMO of CuPc, and the conduction band minimum consists of a group of six states, which are singly, doubly, doubly and singly degenerate, a result of breaking the symmetry of the two sets of three-fold degenerate C_{60} LUMO states. The energy difference between the band extrema, 0.86 eV, is also very close to the value for the molecular complex (0.93 eV). We conclude that optical excitations in the thin film arrangement should be very similar to those in the molecular complex, but the presence of a whole layer of C_{60} molecules would provide an easier pathway for electron transport after the excited electron has been transferred from the CuPc molecule to the nearest C_{60} , and therefore the electron-hole separation should be more effective.

4. Conclusions

We have studied the atomic structure of an isolated CuPc adsorbed on a C_{60} molecule using first-principles calculations. Two classes of configurations, the lying-down (in four arrangements labeled L_{1v} , L_{1c} , L_{1b} , and L_a) and the standing-up orientation (in two arrangements

labeled S_h and S_b), were investigated. The energetically preferred structure is the L_b orientation, which means that a CuPc molecule preferentially adsorbs on the bridge site of the C_{60} surface with one N–Cu–N bond parallel to a C–C bond of C_{60} . For the standing-up orientation, the bridge site is also the energetically favorable adsorption site for the CuPc molecule. The calculated planar averaged charge density differences suggest that the lying-down configurations are more likely to lead to exciton dissociation than the standing-up configurations, because of the larger overlap of the wavefunctions at the CuPc/ C_{60} interface and stronger electron polarization in the former structures. It is interesting that the different molecular orientations in the lying-down or the standing-up configuration do not significantly affect the position and the amplitude of the first absorption peak in the optical spectra.

Based on the investigation of the CuPc/ C_{60} molecular complexes, including atomic structures, and electronic and optical properties, we proceeded to construct models for the heterojunction involving a full CuPc layer on a C_{60} monolayer. We used a square lattice of CuPc molecules lying down on the C_{60} (100) surface and a hexagonal lattice of CuPc molecules standing up on the $C_{60}(111)$ surface. Both systems should be able to form experimentally, depending on the substrate on which the C_{60} layer is deposited (for example, Si(100) or MoS_2 for the (100) orientation and Ag(111) for the (111) orientation of the C_{60} surface). Our results show that the interaction between the two molecular layers is stronger in the CuPc/ $C_{60}(001)$ system than in the CuPc/ $C_{60}(111)$ system. We conclude that the CuPc/ $C_{60}(001)$ thin film heterojunction will exhibit better performance, in comparison to the CuPc/ $C_{60}(111)$ system, because the former should have larger open circuit voltage and stronger electronic interaction between CuPc and C_{60} , leading to easier electron-hole dissociation.

Acknowledgements

We thank Prof. M. Grätzel for helpful discussion. We acknowledge partial financial support from EPFL for J.R., and the National Science Foundation of China (No. 11074287), Ministry of Science and Technology (No. 2012CB921403), and the Hundred Talents program of Chinese Academy of Sciences for S.M.



References

- [1] Hong, Z. R.; Maennig, B.; Lessmann, R.; Pfeiffer, M.; Leo, K.; Simon, P. Improved efficiency of zinc phthalocyanine/C₆₀ based photovoltaic cells via nanoscale interface modification. *Appl. Phys. Lett.* **2007**, *90*, 203505.
- [2] Akaike, K.; Kanai, K.; Ouchi, Y.; Seki, K. Impact of ground-state charge transfer and polarization energy change on energy band offsets at donor/acceptor interface in organic photovoltaics. *Adv. Funct. Mater.* **2010**, *20*, 715–721.
- [3] Ichikawa, M.; Suto, E.; Jeon, H. G.; Taniguchi, Y. Sensitization of organic photovoltaic cells based on interlayer excitation energy transfer. *Org. Electron.* **2010**, *11*, 700–704.
- [4] Tang, C. W. Two-layer organic photovoltaic cell. *Appl. Phys. Lett.* **1986**, *48*, 183–185.
- [5] Chan, M. Y.; Lai, S. L.; Fung, M. K.; Lee, C. S.; Lee, S. T. Doping-induced efficiency enhancement in organic photovoltaic devices. *Appl. Phys. Lett.* **2007**, *90*, 023504.
- [6] Xue, J. G.; Uchida, S.; Rand, B. P.; Forrest, S. R. Asymmetric tandem organic photovoltaic cells with hybrid planar-mixed molecular heterojunctions. *Appl. Phys. Lett.* **2004**, *85*, 5757–5759.
- [7] Kim, J. Y.; Lee, K.; Coates, N. E.; Moses, D.; Nguyen, T. Q.; Dante, M.; Heeger, A. J. Efficient tandem polymer solar cells fabricated by all-solution processing. *Science* **2007**, *317*, 222–225.
- [8] Wang, E. G.; Wang, L.; Lan, L. F.; Luo, C.; Zhuang, W. L.; Peng, J. B.; Cao, Y. High-performance polymer heterojunction solar cells of a polysilfluorene derivative. *Appl. Phys. Lett.* **2008**, *92*, 033307.
- [9] Hiramoto, M.; Sakai, K. Efficient organic p-i-n solar cells having very thick codeposited i-layer composed of highly purified organic semiconductors. *Proc. of SPIE* **2008**, *7052*, 70520H.
- [10] Park, S. H.; Roy, A.; Beaupre, S.; Cho, S.; Coates, N.; Moon, J. S.; Moses, D.; Leclerc, M.; Lee, K.; Heeger, A. J. Bulk heterojunction solar cells with internal quantum efficiency approaching 100%. *Nat. Photonics* **2009**, *3*, 297–302.
- [11] Ray, A.; Goswami, D.; Chattopadhyay, S.; Bhattacharya, S. Photophysical and theoretical investigations on fullerene/phthalocyanine supramolecular complexes. *J. Phys. Chem. A* **2008**, *112*, 11627–11640.
- [12] Huang, H.; Chen, W.; Chen, S.; Qi, D. C.; Gao, X. Y.; Wee, A. T. S. Molecular orientation of CuPc thin films on C₆₀/Ag(111). *Appl. Phys. Lett.* **2009**, *94*, 163304.
- [13] Fendrich, M.; Wagner, T.; Stöhr, M.; Möller, R. Hindered rotation of a copper phthalocyanine molecule on C₆₀: Experiments and molecular mechanics calculations. *Phys. Rev. B* **2006**, *73*, 115433.
- [14] Zhou, Y. C.; Liu, Z. T.; Tang, J. X.; Lee, C. S.; Lee, S. T. Substrate dependence of energy level alignment at the donor-acceptor interface in organic photovoltaic devices. *J. of Electron. Spectrosc. Relat. Phenom.* **2009**, *174*, 35–39.
- [15] Bernède, J. C.; Berredjem, Y.; Cattin, L.; Morsli, M. Improvement of organic solar cell performances using a zinc oxide anode coated by an ultrathin metallic layer. *Appl. Phys. Lett.* **2008**, *92*, 083304.
- [16] Dutton, G. J.; Jin, W.; Reutt-Robey, J. E.; Robey, S. W. Ultrafast charge-transfer processes at an oriented phthalocyanine/C₆₀ interface. *Phys. Rev. B* **2010**, *82*, 073407.
- [17] Huang, Y. L.; Li, H.; Ma, J.; Huang, H.; Chen, W.; Wee, A. T. S. Scanning tunneling microscopy investigation of self-assembled CuPc/F₁₆CuPc binary superstructures on graphite. *Langmuir* **2010**, *26*, 3329–3334.
- [18] Manandhar, K.; Ellis, T.; Park, K. T.; Cai, T.; Song, Z.; Hrbek, J. A scanning tunneling microscopy study on the effect of post-deposition annealing of copper phthalocyanine thin films. *Surf. Sci.* **2007**, *601*, 3623–3631.
- [19] Karacuban, H.; Lange, M.; Schaffert, J.; Weingart, O.; Wagner, Th.; Möller, R. Substrate-induced symmetry reduction of CuPc on Cu(111): An LT-STM study. *Surf. Sci.* **2009**, *603*, L39–L43.
- [20] Godlewski, S.; Tekiel, A.; Prauzner-Bechcicki, J. S.; Budzioch, J.; Szymonski, M. Controlled reorientation of CuPc molecules in ordered structures assembled on the TiO₂(011)-(2 × 1) surface. *ChemPhysChem* **2010**, *11*, 1863–1866.
- [21] Collins, G. E.; Williams, V. S.; Chau, L. K.; Nebesny, K. W.; England, C.; Lee, P. A.; Lowe, T.; Fernando Q.; Armstrong, N. R. Epitaxial phthalocyanine thin films and phthalocyanine/C₆₀ multilayers. *Synth. Met.* **1993**, *54*, 351–362.
- [22] Chen, D.; Sarid, D. Growth of C₆₀ films on silicon surfaces. *Surf. Sci.* **1994**, *318*, 74–82.
- [23] Dresselhaus, M. S.; Dresselhaus, G.; Eklund, P. C. *Science of Fullerenes and Carbon Nanotubes*; Academic Press: San Diego, 1996.
- [24] Troullier, N.; Martins, J. L. Efficient pseudopotentials for plane-wave calculations. *Phys. Rev. B* **1991**, *43*, 1993–2006.
- [25] Ceperley, D. M.; Alder, B. J. Ground state of the electron gas by a stochastic method. *Phys. Rev. Lett.* **1980**, *45*, 566–569.
- [26] Soler, J. M.; Artacho, E.; Gale, J. D.; Garcia, A.; Junquera, J.; Ordejon, P.; Sanchez-Portal, D. The SIESTA method for *ab initio* order-N materials simulation. *J. Phys: Condens. Matter* **2002**, *14*, 2745–2779.

- [27] Dion, M.; Rydberg, H.; Schröder, E.; Langreth, D. C.; Lundqvist, B. I. Van der Waals density functional for general geometries. *Phys. Rev. Lett.* **2004**, *92*, 246401.
- [28] Tsolakidis, A.; Sánchez-Portal, D.; Martin, R. M. Calculation of the optical response of atomic clusters using time-dependent density functional theory and local orbitals. *Phys. Rev. B* **2002**, *66*, 235416.
- [29] Kodama, Y.; Ohno, K. Charge separation dynamics at molecular heterojunction of C₆₀ and zinc phthalocyanine. *Appl. Phys. Lett.* **2010**, *96*, 034101.
- [30] Edwards, L.; Gouterman, M. Porphyrins: XV. Vapor absorption spectra and stability: Phthalocyanines. *J. Mol. Spectrosc.* **1970**, *33*, 292–310.
- [31] Leach, S.; Vervloet, M.; Desprès, A.; Bréheret, E.; Hare, J. P.; Dennis, T. J.; Kroto, H. W.; Taylor, R.; Walton, D. R. M. Electronic spectra and transitions of the fullerene C₆₀. *Chem. Phys.* **1992**, *160*, 451–466.
- [32] Dougherty, D. B.; Jin, W.; Cullen, W. G.; Reutt-Robey, J. E.; Robey, S. W. Striped domains at the pentacene:C₆₀ interface. *Appl. Phys. Lett.* **2009**, *94*, 023103.

